

Development of a Nano-Alumina-Zirconia Composite Catalyst as an Active Thin Film in Biodiesel Production

N. Marzban, J. K. Heydarzadeh M. Pourmohammadbagher, M. H. Hatami, A. Samia

Abstract—A nano-alumina-zirconia composite catalyst was synthesized by a simple aqueous sol-gel method using $\text{AlCl}_3 \cdot 6\text{H}_2\text{O}$ and ZrCl_4 as precursors. Thermal decomposition of the precursor and subsequent formation of $\gamma\text{-Al}_2\text{O}_3$ and t-Zr were investigated by thermal analysis. XRD analysis showed that $\gamma\text{-Al}_2\text{O}_3$ and t-ZrO₂ phases were formed at 700 °C. FT-IR analysis also indicated that the phase transition to $\gamma\text{-Al}_2\text{O}_3$ occurred in corroboration with X-ray studies. TEM analysis of the calcined powder revealed that spherical particles were in the range of 8-12 nm. The nano-alumina-zirconia composite particles were mesoporous and uniformly distributed in their crystalline phase. In order to measure the catalytic activity, esterification reaction was carried out. Biodiesel, as a renewable fuel, was formed in a continuous packed column reactor. Free fatty acid (FFA) was esterified with ethanol in a heterogeneous catalytic reactor. It was found that the synthesized $\gamma\text{-Al}_2\text{O}_3/\text{ZrO}_2$ composite had the potential to be used as a heterogeneous base catalyst for biodiesel production processes.

Keywords—Nano-alumina-zirconia, composite catalyst, thin film, biodiesel.

I. INTRODUCTION

NOWADAYS, several catalytic reactions such as base catalyzed esterification [1]-[3], acid-catalyzed esterification [4], [5], enzymatic esterification [6], [7], and heterogeneous catalyst esterification [8], [9] are used for biodiesel production from FFAs. Now, the homogeneous catalysts are being extensively used for the production of biodiesel at industrial scale such as sulfuric acid, the most common homogeneous catalyst consumed in biodiesel synthesis [10]. The use of the homogeneous catalysts, however, has some disadvantages. One of the most obvious disadvantages of homogenous catalysts is that they should be eliminated from the final product by repeated washing with distilled water, thereby causing the formation of a massive amount of wastewater. In order to overcome such problems, heterogeneous catalysts are applied. Heterogeneous catalysts can be easily separated from the final product and used several times. Alumina is widely used as a catalyst due to its favorable

catalytic properties [11]. In particular, γ -alumina, which has large surface area and suitable pore size distribution, is an important catalyst for binding organic compounds [12].

Zirconia is one of the additives which can increase the strength and toughness of the alumina matrix either by stress-induced transformation toughening or microcrack toughening [13]. Zirconia was selected due to its chemical inertness (compared to other oxide phases), intrinsic catalytic activity (higher than other classical supports like pure Al_2O_3 or SiO_2), and the thermal stability of the $\text{Al}_2\text{O}_3\text{-ZrO}_2$ composite system [14], [15]. On the other hand, it was also shown that alumina delayed the crystallization, increased the specific surface area and pore volume, and enhanced the surface acidity of zirconia [16].

Several methods for the preparation of the alumina-zirconia nanopowders and composites have been reported in the literature [17]-[21]. The sol-gel process is one of the most useful techniques used to offer the possibility of making ultra-homogeneous structures and it has been widely used in the synthesis of glasses, ceramics, and composites catalysts [15], [17]. Sol-gel method is also used for preparing the gels of various shapes such as monoliths, fibers, coating films, spheres, and so on. It is well known that the composition of the starting alkoxide solution including the type of catalyst, water content, the presence or absence of any additives, and the reaction conditions directly affects the rate of hydrolysis, the rate of condensation, the shape of produced polymer particles in the solution, and the state of aggregation of particles, respectively. Thus, characteristics of the sols and gels produced in the reaction could be easily changed by varying several parameters. Sol-gel method, among different coating methods used, has shown promising results due to its low cost, simple control of the synthesized parameters, and the ability to form a uniform coating over large or complex geometric shapes physically and chemically. It has the potential to enhance physical and chemical properties due to the nanocrystalline structure of the coatings [16], [17].

N. Marzban is with the Department of Chemical Engineering, Isfahan University of Technology, Esfahan, Iran (e-mail: n.marzban@ce.iut.ac.ir).

J. K. Heydarzadeh is with the Department of Chemical Engineering, Azad University, Shahrood Branch, Shahrood, Iran.

M. Pourmohammadbagher is with the Department of Chemical Engineering, University of Alberta, Canada.

M. H. Hatami is with Petropishtaz Espadan Company, Esfahan, Iran.

A. Samia is with the Department of Agricultural Biotechnology, Isfahan University of Technology, Esfahan, Iran.

Several investigators have used solutions/sols of alumina and zirconia salts or suspensions of Al_2O_3 and ZrO_2 powders to control the particle size of ZrO_2 and Al_2O_3 [20]. In this research, the sol-gel method was used to synthesize a nano-thin film of alumina-zirconia composite catalysts. Prepared samples obtained through sol-gel technique were then characterized by BET surface area, TEM, XRD, FTIR, and AFM analysis. The purpose of the present research was to develop an effective catalytic process for biodiesel production using nano-alumina-zirconia composite as an active thin film.

II. MATERIALS AND METHODS

A. Preparation of $\text{Al}_2\text{O}_3/\text{ZrO}_2$ Composite Catalyst Thin Film

In order to synthesize $\text{Al}_2\text{O}_3/\text{ZrO}_2$ nanocomposite particles, aluminum chloride hexahydrate ($\text{AlCl}_3 \cdot 6\text{H}_2\text{O}$), zirconium (IV) chloride (ZrCl_4), yttrium (III) nitrate ($\text{Y}(\text{NO}_3)_3 \cdot 6\text{H}_2\text{O}$), citric acid ($\text{C}_6\text{H}_8\text{O}_7$), and ethylene glycol ($\text{HOCH}_2\text{CH}_2\text{OH}$) were prepared by the sol-gel method. All materials were supplied by Merck (Darmstadt, Germany). Fig. 1 shows the stepwise procedures employed for the preparation of the nanocomposite particles and the thin film by the sol-gel method. The mixture of the solutions was relatively stable, i.e., no precipitation or phase separation was observed during the process.

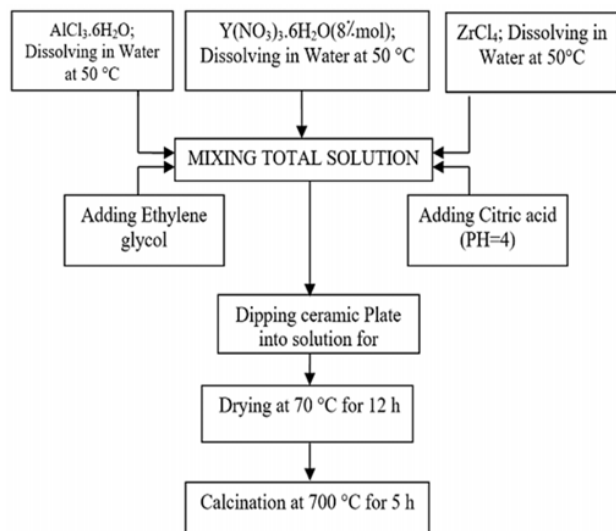


Fig. 1 Typical flow chart of processing nanocomposite $\text{Al}_2\text{O}_3\text{-ZrO}_2$ thin film

Ceramic plates were used as the substrate material. The substrates were coated by dip-coating technique and withdrawn in the solutions at a constant speed of about 1 mm/s. The coated substrates were allowed to be dried at 70 °C for 12 h. The coated plates were then calcinated at 700 °C with a heating rate of 5 °C/min to the distinctive temperature and maintained for 5 h.

B. Catalyst Characterizations

The morphology of the calcinated powders of the thin film was investigated by using a Philips EM208S transmission electron microscope (TEM). For the phase analysis of the thin

film, X-ray diffraction (XRD, Siemens D500 Model) with $\text{Cu-K}\alpha$ radiation in the range of 10–70 and at scanning steps of $2\theta=4$ °/min was used. The crystalline size of the synthesized particle was calculated by using Scherrer's equation as [21]:

$$\frac{0.9\lambda}{B\cos\theta} \quad (1)$$

where D is the crystalline size (nm), λ is the wavelength of X-ray radiation (1.54056 Å), θ is the Berg's angle, and B is the full width at half maximum. The BET surface area of the thin film in air was determined at 700 °C for 5h by a surface analyzer model (Gemini 2375, USA) using N_2 as the adsorbate. Fourier transform infrared spectroscopy (FTIR) analysis of the thin film was carried out in a Nicollet Nexus 6700 spectrometer and in the wave number range of 400-4000 cm^{-1} to study the chemical groups. The surface morphology of the thin film was examined by an Auto Probe model CP atomic force microscope (AFM, Park scientific instruments, USA) using a Si_3N_4 probe.

C. Reaction Test

The esterification process was carried out in a continuous packed bed reactor. The column was packed and loaded with palletized catalysts (600 g, $\gamma\text{-Al}_2\text{O}_3/\text{ZrO}_2$). About 82% of the reactor volume was occupied by the palletized catalysts. The schematic diagram for the experimental setup is shown in Fig. 2. Fatty acids mixture and ethanol were primarily heated up to 50 °C in a mixing tank. The fatty acids were pumped to the top of the column. The FFA met and interacted with ethanol on the active sites of catalysts, and the ester product was instantaneously formed. The product was transferred to a flash drum separator [22].

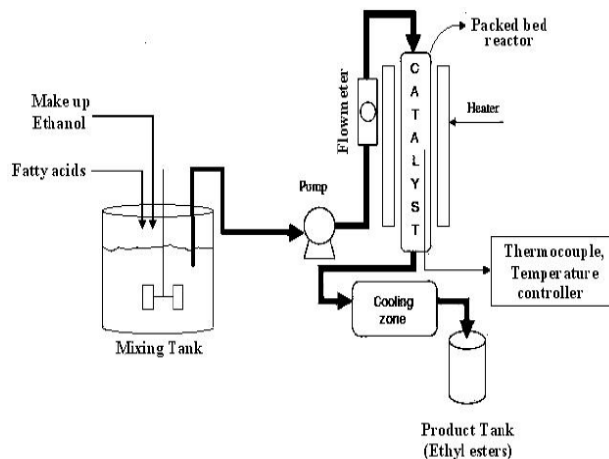


Fig. 2 Schematic diagram of the experimental setup

III. RESULTS AND DISCUSSION

A transmission electron microscope (TEM) was used to analyze the particle size and morphology of the nanocomposite powder particles. Fig. 3 shows the micrograph of alumina-zirconia composite powders synthesized using sol gel method and calcinated at 700 °C for 5 h. Most particles were in the range of 10-15 nm. The phenomenon of meso-porosity within

particles could also be observed in this TEM picture, and most particles were spherical in nature. TEM studies showed powder agglomeration. Generally, it can be said that the increase in specific surface area may improve the catalytic activity. The specific surface area of the final composite powders was determined by the BET surface area analysis, and the calculated surface area was about $\sim 120 \text{ m}^2/\text{g}$.

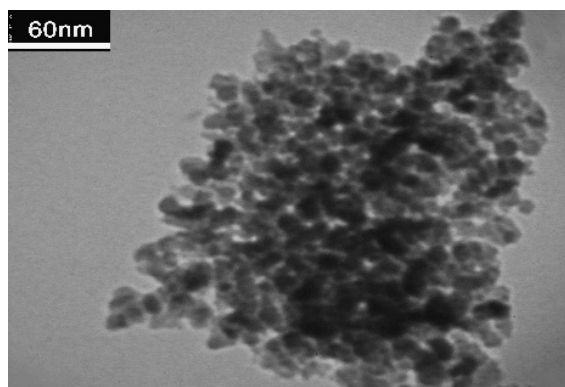


Fig. 3 Transmission electron micrographs of the alumina-zirconia particles after calcination at 700°C for 5h

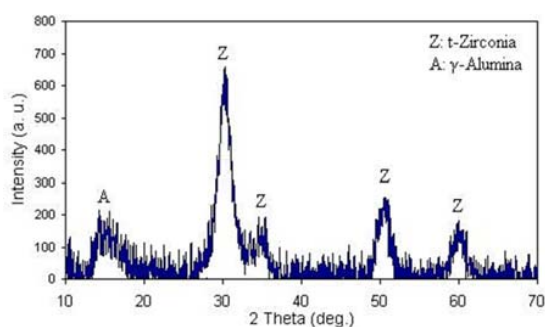


Fig. 4 Phase analysis of the synthesized coating after calcination at 700°C

The X-Ray diffraction pattern has been shown in Fig. 4. It indicated that the calcined coating seemed to be amorphous. This might be due to the organic compounds of the coating. The strong peak at $2\theta=30.2^\circ$ was assigned to the (111) lattice plan whereas the other weak peak at $2\theta=35.11^\circ$, 50.65° , 60.17° , and 63.10° could be ascribed to (200), (220), (131), and (222) lattice planes of tetragonal Zirconia ($t\text{-ZrO}_2$) phase, respectively. The stabilization of $t\text{-ZrO}_2$ could be attributed to the structural similarity of the dopant, Y_2O_3 , ZrO_2 , and the larger dopant cation radius compared with the Zr^{4+} radius [23]. The yttria was changed into yttrium oxide when exposed to the high temperature (700°C). Another explanation for the stabilization of the tetragonal phase of zirconia in Y_2O_3 doped ZrO_2 system could be based on the formation of oxygen vacancies resulting from the presence of trivalent cation [24], [25]. Also, the strong peak at $2\theta=14.7^\circ$ was assigned to the lattice plan whereas the other weak peak at $2\theta=54.2^\circ$, and 55.3° could be ascribed to the lattice planes of $\gamma\text{-Al}_2\text{O}_3$. It can be concluded that the prepared nanopowders have obviously different crystal structures. The

alumina was diffused into the zirconia lattice, stabilizing the crystal phase of zirconia in the sample. The broadening of peaks in XRD pattern confirmed that the average crystallite size was small. The crystallite size of the calcined powder was calculated by using Scherrer's equation, and the size varied between 5 nm and 15 nm.

FTIR analysis for the synthesized composite in the wave number region of $4000\text{-}400 \text{ cm}^{-1}$ is shown in Fig. 5. The band located at $\sim 3440 \text{ cm}^{-1}$ was attributed to the O-H stretching vibration and the band at $\sim 1640 \text{ cm}^{-1}$ was related to the H-O-H symmetric stretching vibration of adsorbed water molecules. The absorption bands centered at ~ 600 and $\sim 800 \text{ cm}^{-1}$ were assigned to the Al-O bonding vibration in tetrahedral and octahedral environments respectively, suggesting γ -alumina [26]. Also, the band at 480 cm^{-1} corresponded to the vibration absorption of Zr-O bond in tetragonal zirconia. This can be explained by the relative contribution of two bonds, Zr-O and Al-O bonds, and it is consistent with the formation of $\text{ZrO}_2\text{-Al}_2\text{O}_3$. This supports the XRD results and the formation of alumina and zirconia in the present study.

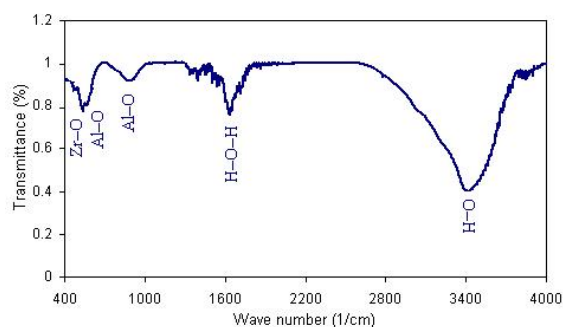


Fig. 5 FTIR curves of $\text{Al}_2\text{O}_3/\text{ZrO}_2$ coating after calcination at 700°C

AFM images of the thin coating $\text{Al}_2\text{O}_3/\text{ZrO}_2$ composite on the ceramic plate are shown in Fig. 6. It demonstrated that the surface of the alumina-zirconia coating was compact. The coating was crack-free and consisted of nanoscale crystallites. However, the surface of the coated $\text{Al}_2\text{O}_3/\text{ZrO}_2$ composite was uneven and sin used, but the roughness of the catalyst was less than 10 nm.

A. Esterification Reactions

The rate of esterification was strongly influenced by the mass ratio of fatty acid to ethanol. Since the esterification process was reversible, the yield of ethyl esters produced was favored with the excess amount of ethanol. In order to obtain an optimal mass ratio for this process, five experiments were carried out with variable FFA/ethanol mass ratios, between 1:5 and 3:5.

Fig. 7 shows the conversion of FFA to ethyl ester as a function of the mass ratio of FFA/ETOH. However, the presented data demonstrated that at a mass ratio of 3:5, the maximum ester yield was obtained. Increasing the mass ratio from 1:1 to 3:5 raised the conversion of ester formation from 25 to 90%. Also, ethyl ester formation was strongly dependent on the reaction temperature.

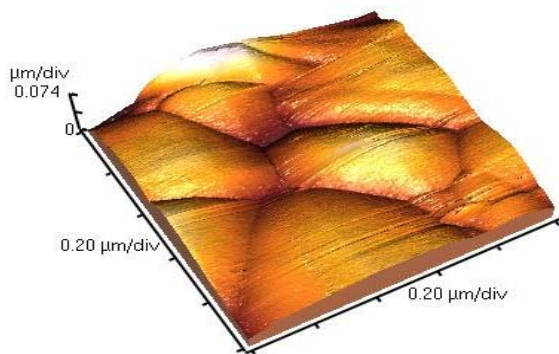


Fig. 6 AFM images of coating $\text{Al}_2\text{O}_3/\text{ZrO}_2$ composite on the ceramic plate

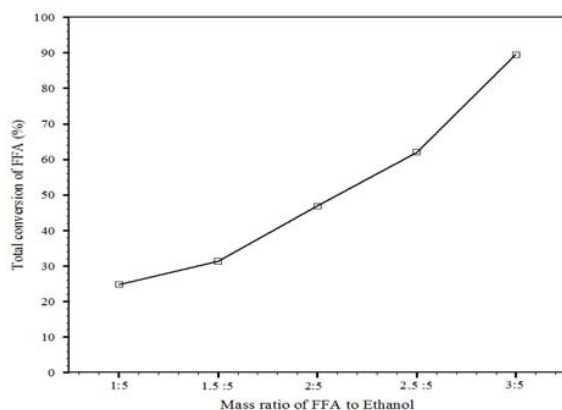


Fig. 7 Conversion of FFA to ethyl ester as a function of the mass ratio of FFA/ETOH

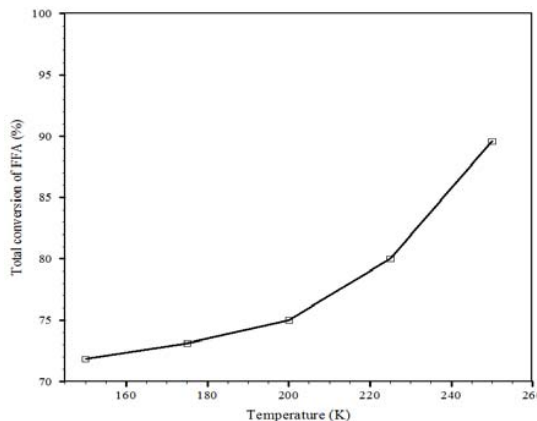


Fig. 8 The effect of temperature on the yield of ethyl ester

To evaluate the effect of reaction temperature on the production of ethyl esters, the esterification process was carried out under optimal conditions. Esterification could be conducted at various temperatures. In most cases, the temperature has been kept close to the boiling point of alcohol used in the process [27]. However, high temperatures can reduce the reaction time. In this research, temperature was varied in the range of 150–250 °C. As shown in Fig. 8, the results indicated that increasing the

reaction temperature had a favorable influence on the yield of ethyl ester formation.

IV. CONCLUSIONS

In this study, we intended to examine a new heterogeneous base composite catalyst in order to develop an effective catalyst for biodiesel production. A novel sol–gel technique was developed in which the alumina and zirconia sol could be prepared at room temperature from the inorganic salts. This process could be used to prepare uniform mesoporous alumina-zirconia composites. The present work demonstrated the manufacture of a nano-film $\gamma\text{-Al}_2\text{O}_3\text{-ZrO}_2$ composite coated on ceramics plates through the sol–gel route. The heterogeneous catalytic reactor had a great ability to produce biodiesel fuel within a short reaction time. It could be concluded that as the mass ratio of FFA/ethanol was increased, the reaction yield and conversion of FFA were increased. The maximum reaction yield at the mass ratio of 3:5 was 90%. At the high temperature (250 °C), high reaction conversion was reached. As expected, at the low temperature, the conversion was low. With the implementation of optimal operational condition, the maximum yield of approximately 90% was achieved. These results showed the possibility for this composite catalyst to act as an effective heterogeneous base catalyst for the manufacture of biodiesel.

REFERENCES

- [1] Leung, D.Y.C., Wu, X. and Leung, M.K.H. (2010). A review on biodiesel production using catalyzed transesterification, *Applied Energy*, 87(4): 1083-1095.
- [2] Liu, X., He, H., Wang, Y., Zhu, S. and Piao, X. (2008). Transesterification of soybean oil to biodiesel using CaO as a solid base catalyst, *Fuel*, 87(2): 216-221.
- [3] Lam, M.K., Lee, K.T. and Mohamed, A.R. (2010). Homogeneous, heterogeneous and enzymatic catalysis for transesterification of high free fatty acid oil (waste cooking oil) to biodiesel: A review, *Biotechnology Advances*, 28(4): 500-518.
- [4] Miao, X., Li, R. and Yao, H. (2009). Effective acid-catalyzed transesterification for biodiesel production, *Energy Conversion and Management*, 50(10): 2680-2684.
- [5] Jain, S. and Sharma, M. (2010). Kinetics of acid base catalyzed transesterification of *Jatropha curcas* oil, *Bioresource technology*, 101(20): 7701-7706.
- [6] Ognjanovic, N., Bezbradica, D. and Knezevic-Jugovic, Z. (2009). Enzymatic conversion of sunflower oil to biodiesel in a solvent-free system: process optimization and the immobilized system stability, *Bioresource technology*, 100(21): 5146-5154.
- [7] Shah, S. and Gupta, M.N. (2007). Lipase catalyzed preparation of biodiesel from *Jatropha* oil in a solvent free system, *Process Biochemistry*, 42(3): 409-414.
- [8] Kim, H.J., Kang, B.S., Kim, M.J., Park, Y.M., Kim, D.K., Lee, J.S. and Lee, K.Y. (2004). Transesterification of vegetable oil to biodiesel using heterogeneous base catalyst, *Catalysis Today*, 93(315-320).
- [9] Xie, W. and Li, H. (2006). Alumina-supported potassium iodide as a heterogeneous catalyst for biodiesel production from soybean oil, *Journal of Molecular Catalysis A: Chemical*, 255(1-2): 1-9.
- [10] Lopez, D.E. and Goodwin, J.G. (2005). Transesterification of triacetin with methanol on solid acid and base catalysts, *Applied Catalysis A: General*, 295(2): 97-105.
- [11] Marandi, V. and Najafpour, G.D. (2001). Reaction rate model for diethyl ether from ethanol using heterogeneous catalysts, *International Journal of Engineering Science and Technology*, 12:1-10.
- [12] Liu, Q., Wang, A., Wang, X., Gao, P., Wang, X. and Zhang, T. (2008). Synthesis, characterization and catalytic applications of mesoporous³-

- alumina from boehmite sol, *Microporous and Mesoporous Materials*, 111(1-3): 323-333.
- [13] Sarkar, D., Mohapatra, D., Ray, S., Bhattacharyya, S., Adak, S. and Mitra, N. (2007). Synthesis and characterization of sol-gel derived ZrO₂ doped Al₂O₃ nanopowder, *Ceramics international*, 33(7): 1275-1282.
- [14] Dominguez, J., Hernandez, J. and Sandoval, G. (2000). Surface and catalytic properties of Al₂O₃-ZrO₂ solid solutions prepared by sol-gel methods, *Applied Catalysis A: General*, 197(1): 119-130.
- [15] Enache, D., Roy-Auberger, M., Esterle, K. and Revel, R. (2003). Preparation of Al₂O₃-ZrO₂ mixed supports; their characteristics and hydrothermal stability, *Colloids and Surfaces A: Physicochemical and Engineering Aspects*, 220(1-3): 223-233.
- [16] Feth, M.P., Bauer, M., Kickelbick, G., Metelkina, O., Schubert, U. and Bertagnolli, H. (2005). Influence of additives and post-synthesis treatment on the structural properties of sol-gel prepared alumina-doped zirconia studied by EXAFS-spectroscopy and X-ray diffraction, *Journal of non-crystalline solids*, 351(5): 432-443.
- [17] Khalil, N., Hassan, M., Ewais, E. and Saleh, F. (2010). Sintering, mechanical and refractory properties of MA spinel prepared via co-precipitation and sol-gel techniques, *Journal of Alloys and Compounds*, 496(1-2): 600-607.
- [18] Jayaseelan, D.D., Rani, D.A., Nishikawa, T., Awaji, H. and Gnanam, F. (2000). Powder characteristics, sintering behavior and microstructure of sol-gel derived ZTA composites, *Journal of the European Ceramic society*, 20(3): 267-275.
- [19] Bartolomé, J.F., Pecharrón, C., Moya, J.S., Martín, A., Pastor, J.Y. and Llorca, J. (2006). Percolative mechanism of sliding wear in alumina/zirconia composites, *Journal of the European Ceramic society*, 26(13): 2619-2625.
- [20] Weng, M.T., Wei, W.C.J. and Huang, C.Y. (2007). Influence of 3Y-TZP on Microstructure and Mechanical Properties of Al₂O₃-based Composites, *Key Engineering Materials*, 353(1540-1543).
- [21] Klug, H.P. and Alexander, L.E. (1974). *X-Ray Diffraction Procedures: For Polycrystalline and Amorphous Materials*, 2nd Edition, 992, Wiley-VCH.
- [22] Heydarzadeh, J.K., Amini, G., Khalizadeh, M.A., Pazouki, M., Ghoreyshi, A.A., Rabiee, S.M. and Najafpour, G.D. (2010). Esterification of Free Fatty Acids by Heterogeneous γ -Alumina/Zirconia Catalysts for Biodiesel Synthesis, *World Applied Science Journal*, 9(11): 1306-1312.
- [23] Del Monte, F., Larsen, W. and Mackenzie, J.D. (2000). Chemical interactions promoting the ZrO₂ tetragonal stabilization in ZrO₂-SiO₂ binary oxides, *Journal of the American Ceramic Society*, 83(6): 1506-1512.
- [24] Das, D., Mishra, H., Parida, K. and Dalai, A. (2002). Preparation, physico-chemical characterization and catalytic activity of sulphated ZrO₂-TiO₂ mixed oxides, *Journal of Molecular Catalysis A: Chemical*, 189(2): 271-282.
- [25] Raz, S., Sasaki, K., Maier, J. and Riess, I. (2001). Characterization of adsorbed water layers on Y₂O₃-doped ZrO₂, *Solid State Ionics*, 143(2): 181-204.
- [26] Macedo, M.I.F., Osawa, C.C. and Bertran, C.A. (2004). Sol-gel synthesis of transparent alumina gel and pure gamma alumina by urea hydrolysis of aluminum nitrate, *Journal of sol-gel science and technology*, 30(3): 135-140.
- [27] Fernando, S., Karra, P., Hernandez, R. and Jha, S.K. (2007). Effect of incompletely converted soybean oil on biodiesel quality, *Energy*, 32(5): 844-851.